WEAR MECHANISMS AND IN-SERVICE SURFACE MODIFICATIONS OF A STELLITE 6B CO-CR ALLOY

E. Bemporad, M. Sebastiani, V. Mangione, D. De Felicis, and F. Carassiti

University of Rome "ROMA TRE", Engineering Department
Via della Vasca Navale 79, 00146 Rome, Italy

Abstract: In the present paper, the in-service wear mechanisms and cross-sectional microstructural evolution of a Stellite 6B cobalt-based alloy subjected to sliding contact conditions are analysed. The analysis is carried out using focused ion beam (FIB), transmission electron microscopy (TEM), 3D confocal profilometer and nanoindentation techniques. Samples under investigation consisted of a lip-seal adopted in a Tunnel Boring Machine (TBM). In the working conditions, the lip-seal is in sliding contact with a rubber seal in a pressurised oil environment. In those conditions, an unexpected low wear resistance was observed during service. As a consequence, a long machine downtime was necessary to replace the damaged component. Results of FIB-SEM/EDS characterisation showed severe grooving due to the presence of sand (SiO_2) particles embedded in the rubber seal in the contact area. In addition, three body abrasive wear is observed immediately outside the contact area. Microstructural evaluation of Stellite 6 B Co-based alloy of the cross-section also showed the presence of a nano-crystalline hardened layer with diffuse presence of stacking faults. The presence of a tribo-film with a complex structure was also clearly observed. It is concluded that wear resistance of such components could be significantly enhanced either by a proper control of abrasive contaminant particles in the lubricant oil or by introducing a proper protective coating (e.g. a thermal sprayed thick coating).

Keywords: abrasive wear, Stellite, FIB, TEM, nanoindentation

1. INTRODUCTION

Cobalt-based "Stellite" alloys are commonly used as hard-facing materials in a variety of industrial applications, as they possess high hardness at high temperature, good resistance to sliding wear under elevated contact pressure and good corrosion resistance [1-3]. The typical microstructure of such alloys [4-7] consists of hard carbides dispersed in a cobalt-rich solid solution matrix.

Depending on the severity of the contact, nature of the counterpart, lubrication conditions and other in-service environmental conditions, different mechanisms of surface modification in tribological contacts have been identified in the literature, either involving or not involving material transfer to the worn surface. Among others, the most important ones are surface hardening, fatigue cracking, phase transitions, diffusion, chemical reactions and formation of tribo-film [8-9].

On the other side, conventional sample preparation techniques on worn surfaces often introduce artefacts; thus hiding the tribological film structures and causing uncertainty in the analyses of near-surface layers. To solve this problem, Focused Ion Beam (FIB and TEM) techniques [10-13] have been recently proposed for the high resolution three-dimensional characterization of worn surfaces.

All these observations suggest that (i) a complete knowledge of actual surface morphology and microstructure is absolutely necessary for a correct design of components subject to mechanical wear, (ii) post-test evaluation of both surfaces and cross-section should be performed with the highest accuracy and (iii) the use of high resolution microscopy techniques should be applied successfully to the characterization of in-service wear behaviour of advanced materials, especially when component failure can lead to long and expensive machine downtime.

In the present paper, focused ion beam (FIB) techniques and TEM observations are proposed for the analysis of the in-service wear behaviour of large-scale components made of a Stellite 6B alloy for heavy duty industrial use.

2. EXPERIMENTAL DETAILS

The analysed worn component consisted of a lip-seal (6.8 m diameter) adopted in a Tunnel Boring Machine (TBM) used for tunnel construction. The lip-seal is produced by bending and subsequent welding of four Stellite 6B annealed plates. The component also undergoes a further finishing (grinding) process. This process could also induce a surface hardened layer and a residual stress state at the material surface.

In the actual tribosystem, the lip-seal is in sliding contact with a rubber seal (a nitrile rubber with CaCO3 filler) at three different points. In the correspondence of the contact points, the oil pressure is progressively increasing (see Fig. 1a, the milling head of TBM rotates around x axis, a schematic detail of the system is reported). Pressurised grease is also present to guarantee the insulation between the milling head and the leap-seal (see Fig. 1a). Nonetheless, it is likely that some SiO2 particles coming from the milling process and present inside the grease could reach the contact areas.

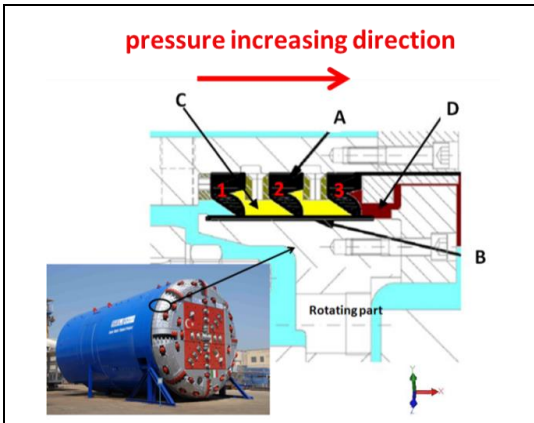

Fig. 1a - Schematic section of the analysed Tunnel Boring Machine (TBM) - lip-seal zone, the blue colour represents air. A: rubber seals; B: Stellite lip-seal; C pressurized oil; D pressurized grease.

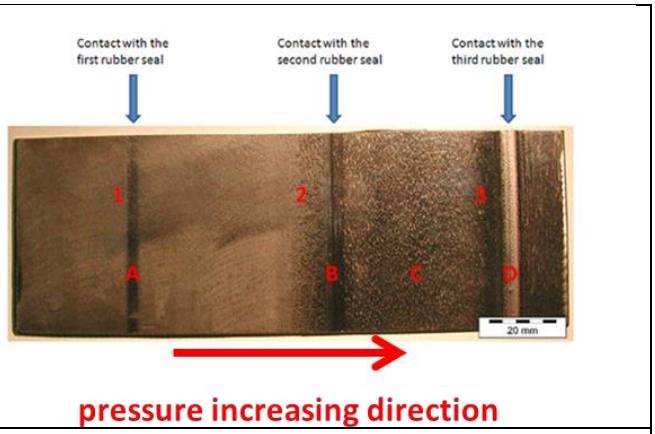

Fig. 1b Worn surface in correspondence of the contact areas

The two samples under investigation were cut from (I) an unbent annealed plate (Stellite 6B annealed as supplied) named sample A and (II) a worn component subject to in service conditions (6 rpm at 50°C) for 8000 h named sample B and showed in Fig. 1b.

The mechanical characterization of both samples was performed by nanoindentation testing [14-15], using the grid indentation technique [16-17] applied on the top mirror polished surface for sample A and on a cross section polished surface for sample B.

The morphology of the worn surfaces was analysed by in-plane Scanning Electron Microscopy (SEM) techniques, coupled with Energy Dispersive Spectroscopy for the compositional analysis (not reported in this work).

3D investigation of the worn surfaces was carried out by a non-contact profilometer in confocal mode.

Microstructural evaluation was performed by FIB both in the worn surfaces and outside the wear track.

Finally, in order to investigate the presence of tribolayers and/or structural/compositional modifications that could have affected the in-service wear behaviour of the component, a TEM lamella was extracted from the centre of the deepest wear track.

Worn components subject to in service conditions (6 rpm at 50°C) for 8000 h were analysed in order to have direct information about their actual wear behaviour.

3. RESULTS

The microstructure of the Stellite alloy under investigation (as-received, i.e. not processed by bending and finishing) is reported in Fig. 2a. There, the presence of coarse chromium carbides in a cobalt matrix is observed and the nanoindentation grid is recognisable. Figure 2b shows the corresponding 2D hardness map.

A good agreement was found between the two images (Figs. 2a and 2b), clearly confirming the difference in terms of hardness that exists between the two phases.

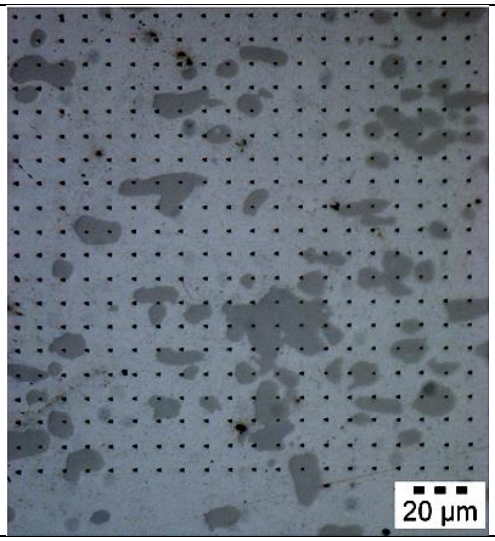

Fig. 2a Area of the nanoindentation grid on annealed Stellite 6B alloy plate

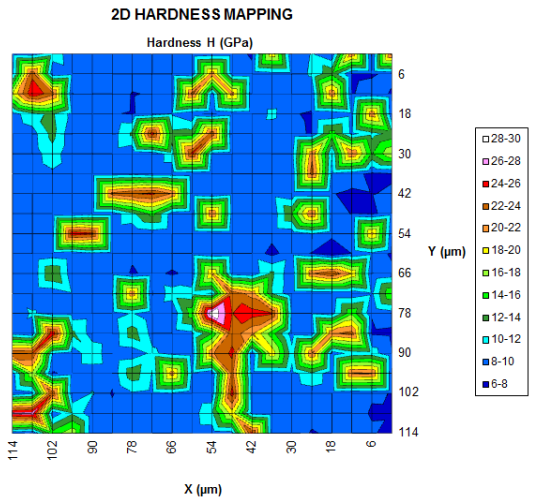

Fig 2b 2D hardness map obtained by the nanoindentation grid

Elastic modulus of the Co-based metal matrix (GPa)	266,6 ± 5,37
Nano-hardness of the Co-based metal matrix (GPa)	8,70 ± 0,35
Elastic modulus of the hard phase (carbides) (GPa)	346,7 ± 6,3
Nano-hardness of the hard phase (carbides) (GPa)	24,30 ± 0,28
In service wear rate** (m^3/m·N)	$3.13 \cdot 10^{-15}$

Table I. mechanical properties and wear rate obtained for sample B.

As showed in Table I, the hardness of the carbide phase was found to be of the order of 24.3 ± 0,28 GPa, while a value of about 8.7 ± 0,35 GPa was found for the Co-based metal matrix. However, it can be clearly noticed that the composite material also shows regions of measured hardness down to 6 GPa.

The wear rate corresponding to the deeper track (track 3 in Fig.1b) was evaluated by the Archard's law [18], assuming the main contact pressure to be equal to the yield strength of the rubber seals (7 MPa) and a sliding distance of about $3 \cdot 10^7$ m. This value is significantly higher than other values that can be found in the literature for similar materials and testing conditions [4-7].

It is worth noting that the morphology of the worn surfaces is completely different in the three contact areas,.[20]. This can be related with the different oil and grease pressure existing between the seals and with the amount and dimension of the abrasive particles, these coming from the environment during the digging operation of the machine. This abrading media (i.e. oil or grease and solid particles), caused severe plastic deformation along the direction of sliding (Fig. 3c and 3d). In particular, the deepest wear track can be found in correspondence of the third rubber seal (labelled 3 in Fig.1b) close to the area with the highest pressure, where the presence of abrasive particles (revealed as SiO2 form EDS analysis) is more probable. An extensive abrasive wear is observed outside the contact area (see Fig. 1b, on the left of wear track 3).

Severe grooving abrasions are visible in the area of contact (Figure 3d), and in its vicinity (Figure 3c). The grooving is probably due to the abrading particles embedded in the rubber seal.

In the wear tracks 1 and 2 there are not evident plastic deformations, while some grooves are present along the sliding direction, due to the presence of fewer or smaller particles of SiO2.

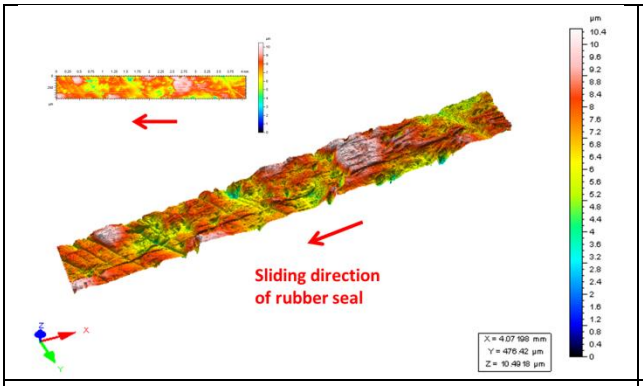

Fig. 3a: 3D profilometric image of wear track 1

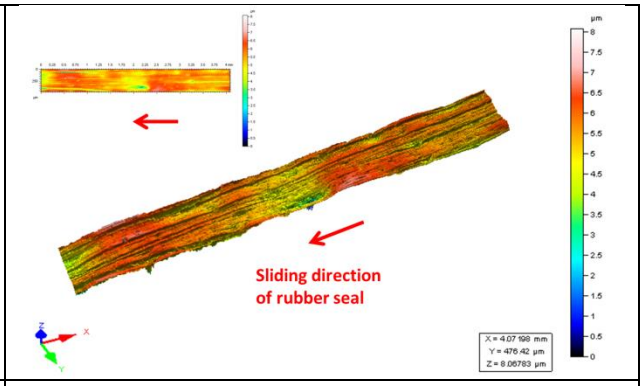

Fig. 3b: 3D profilometric image of wear track 2

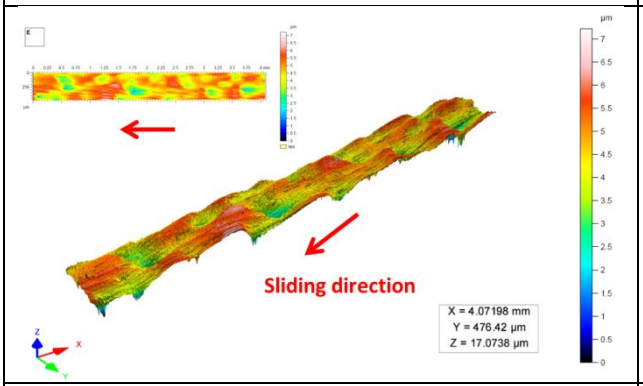

Fig. 3c: 3D profilometric image between wear track 2 and 3

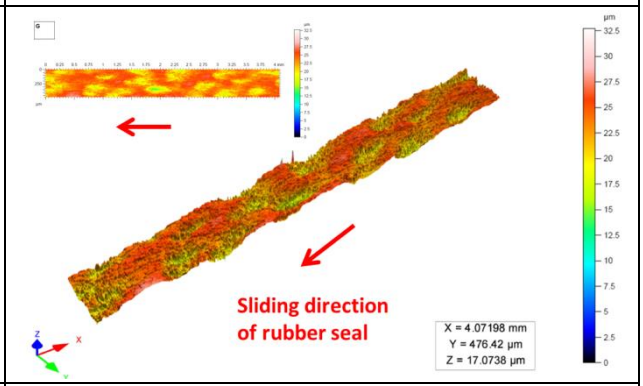

Fig. 3d: 3D profilometric image of wear track 3

Figure 4a shows FIB sections of sample A, presenting a coarse grains microstructure with no hardened layer.

On the other hand, a 2 µm thick surface hardened layer is clearly visible in sample B, even if it is far from the worn surfaces (on the left of wear track 1, see Fig. 1b), (Figure 4b). This is probably due to the shaping (i.e. rolling) and grinding processes, which changes considerably the surface microstructure and its tribo-mechanical behaviour.

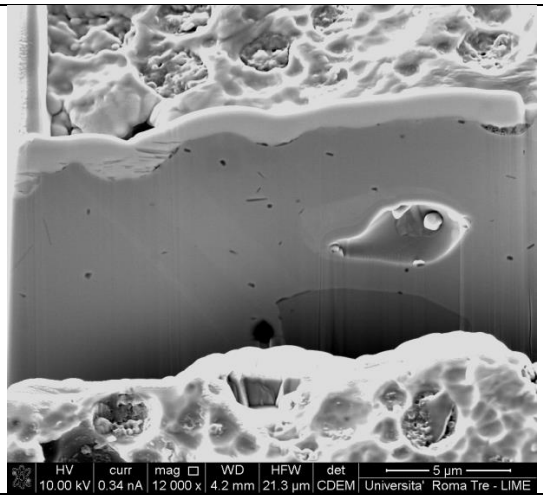

Fig. 4a FIB section of the as received annealed Stellite 6B alloy plate

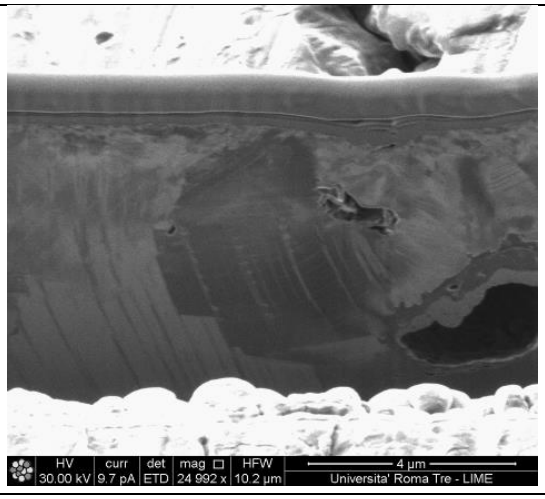

Fig. 4b FIB section outside the worn surface

Microstructural evaluations of the cross-section performed by FIB on worn surfaces are reported in Figures 5a-b (outside the contact area between track 3 and 2) and Figures 6a-d (inside the contact area, i.e. inside the track 3), where significant surface modifications and the formation of a tribolayer are observed at the specimen surface, especially near the carbide/matrix interfaces.

In particular, a ca. 2µm deep hardened micro/nano-crystalline layer is formed in the matrix at the very surface, while a significant amount of stacking faults and shear bands (highlighted by arrows in figs. 5a-b) is observed in the subsurface layers.

It is important to note that the average depth of wear track 3 was greater than 1 mm, and this demonstrates that the hardened layer cannot be due to the preliminary grinding process but it is essentially due to severe plastic deformation during in-service wear.

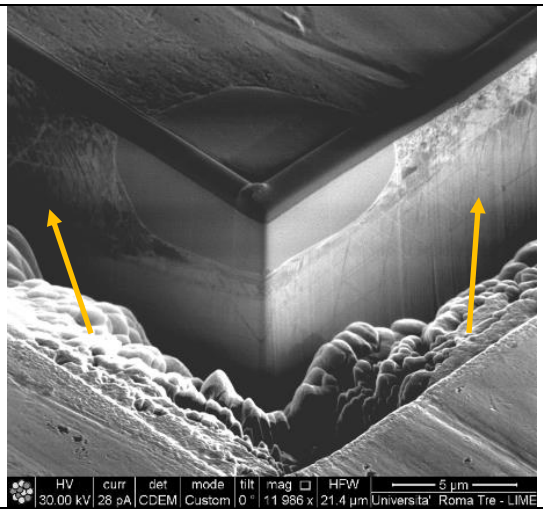

Fig. 5a FIB section of the worn surface outside the contact area (arrows indicate the hardened layer)

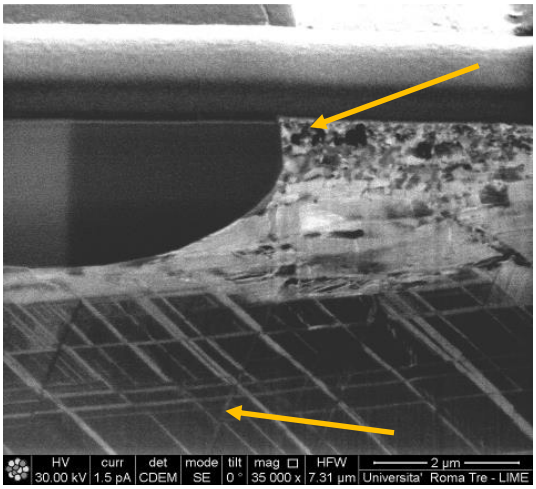

Fig. 5b FIB section of the worn surface outside the contact area – detail (arrows indicate the hardened layer and stacking faults)

It is also worth mentioning that similar deformation mechanisms are observed both inside (Figures 6a-b) and outside (Figures 5a-b) the contact area, suggesting that the hardened layer is given by the action of the abrading particles coming from the operation of the machine while digging.

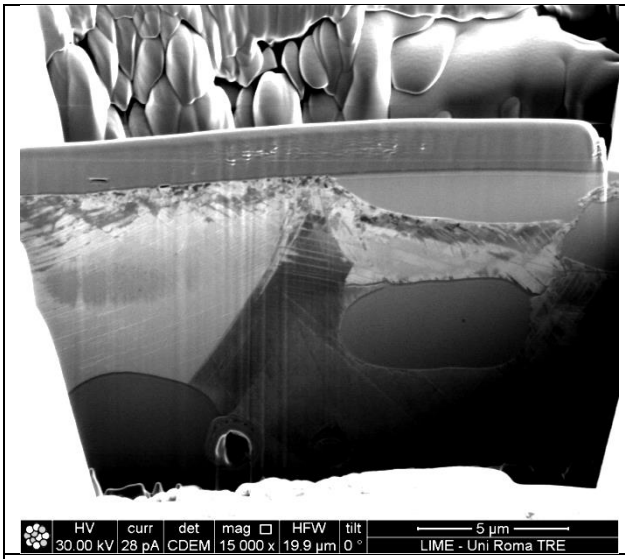

Fig. 6a FIB section of the worn surface inside the contact area

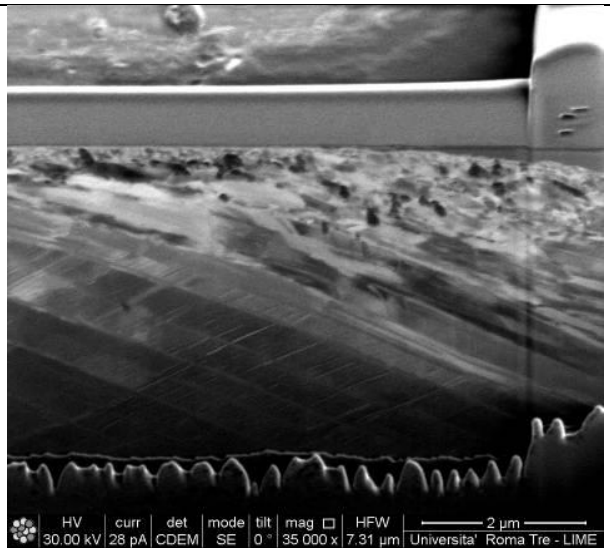

Fig. 6b FIB section of the worn surface inside the contact area – detail

A more detailed TEM-SAED analysis of the worn surface is reported in Figure 7a-b, where three different areas are identified in the plastically deformed zone: (1) a nano-crystalline 100 nm thick layer at the very surface, (2) a 300 nm micro-crystalline layer with a significant presence of shear bands

and (3) a crystalline layer where the deformation effects only consist of shear bands of stacking faults. A complete re-crystallization during plastic deformation is observed in zones (1) and (2), as it is clearly visible in Figure 7b, where a detail of the nano-crystalline surface layer and related SAED pattern are reported.

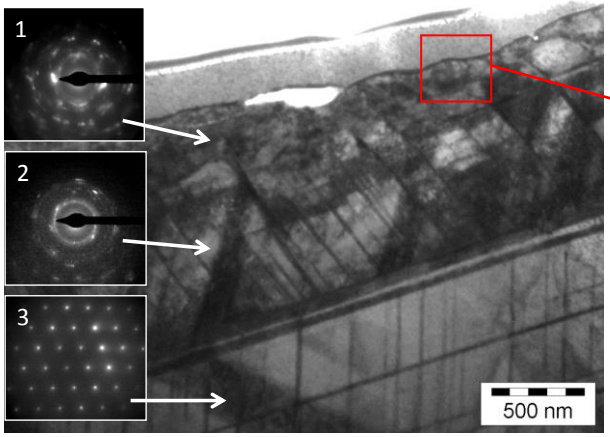

Fig. 7a TEM-SAED analysis, showing a transition from a nano-crystalline microstructure at the surface to the pristine crystalline inner layers.

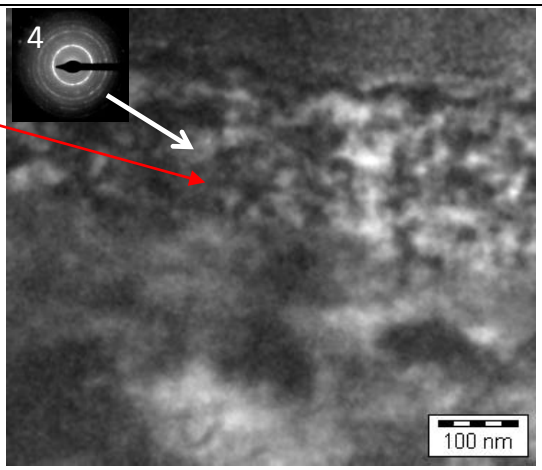

Fig. 7b detail of the surface nano-crystalline tribolayer

4. DISCUSSION

The main purpose of the present paper was to understand the in-service modifications and wear mechanisms of a Stellite 6B lip-seal, by the use of use FIB/SEM-TEM microscopy and to give further insights into the actual in-service wear mechanisms of large-scale Stellite-alloy components.

The use of FIB/SEM techniques was effective in providing an explanation for the high wear rate observed for this component. in comparison with literature data found in the literature [4-7] in fact, the wear rates were significantly higher, especially for the case of pure sliding wear.

The microstructural cross-section analysis of worn surfaces clearly showed that complex surface modifications occurred during wear. In particular, the formation of a thin nano-crystalline hardened layer was observed at the specimen surface. FIB-SEM and EDS analyses (not reported in this paper) also showed the presence of an iron-rich tribolayer on the carbide grains and SiO2 contaminants embedded in the Co-rich matrix. Plastic deformation was shown by profilometric analysis, especially in the area with higher contact pressure, where the hardened layer is also characterized by stacking fault formation. A clear and stepwise transition from a nano-crystalline microstructure to the pristine crystalline one was observed from the surface down to the inner layers (Figures 7a-b).

All these observations suggest that different concurrent phenomena contribute to the observed deformation mechanisms, in particular: (a) the action of small (micron size) abrading particles give rise to local surface plastic deformation and to severe localised wear which involved the complete recrystallization at specimen surface and the formation of a nano-crystalline layer at the very surface; (b) the action of larger particles gives rise to a less severe in-bulk plastic deformation, mainly based on stacking fault formation, which is localised at a deeper depth due to the higher contact radius of the particles.

A final point to be discussed is the reliability of nanoindentation test data and some further information that can be derived from the hardness map. The presence of edge effects is clearly visible in Figure 2b: an increment of hardness of the matrix is present in the proximity of carbide grains (green and light blue in the contour plot). These effects can be explained respectively with the severe work hardening of the Co phase nearby the carbides, as confirmed by FIB analyses.

5. CONCLUSIONS

In the present paper, the wear behaviour of a cobalt base wear-resistant alloy (Stellite 6B) under in-service wear conditions was analysed using high resolution microscopy techniques (FIB-SEM/TEM).

In-plane and cross-section microstructural analyses suggest that the in-service wear behaviour of the analysed components is deeply modified by the presence of SiO2 and Fe contaminations inside the lubricating oil, leading to severe two-body grooving wear inside the contact area and to three body abrasive wear outside the contact area.

A hardened nano-crystalline layer with diffuse presence of stacking faults was observed, while the benefic effect given by the carbide grains could be significantly enhanced by obtaining a much finer dispersion of the second phase.

These results lead to the conclusion that the wear mechanisms of the component likely consist of a mixture of two-body grooving and three body abrasive wear of the cobalt-rich matrix, due to the action of Fe and SiO2 particles coming from the drilling process and dispersed in the lubricating oil and grease. Therefore, the analysis performed shows that the wear resistance of such components could be significantly improved by limiting the presence of the abrading particles inside the lubricant oil or, if this cannot be possible due to design limitations, by the adoption of a different facing material of the lip seal itself. The role of the ratio between the size of the carbide grains and the size of the abrading particles is of capital importance and shall be carefully considered while designing composite materials subjected to sliding wear. In fact, this ratio enabled the CoCr matrix to dominate the wear behaviour through removal/displacement of CoCr matrix material. In this case, the matrix is significantly softer than the silica abrading particles (Fig 2a and Fig 2b), thus leading to its rapid and unmanageable wear.

The analysis of in service wear behaviour was therefore useful in this situation, because of the significant differences on both (i) the starting material that undergoes wear (surface hardened layer and residual stress due to the preliminary grinding of the component) and (ii) the actual in-service lubrication conditions, in comparison to what is usually obtained at a lab-scale.

The use of a more highly work-hardened surface layer in the CoCr matrix, or a much finer microstructure for the same alloy, would be unlikely to resist this form of abrasion. In fact, in the conditions analysed, the hardness of the contaminating particles plays the more important role in determining the wear process.

In perspective, a much more effective solution could be obtained by the adoption of nano-structured multiphase hard-facing alloys. As an example, a WC-Co nanostructured HVOF coating [18-19] could be a more suitable solution for this specific situation. In fact, under these specific in-service environmental conditions, a high proportion of WC is usually present and a very fine dispersion of the hard particle is achieved by nanostructuring. Another possible solution could be the use of the laser cladding coating technique [2,7], which is commonly adopted to obtain thick films of a variety of hard materials, including Co alloys. The adoption of a thick coating seems to be a suitable solution in view of the improvement of performances of such large-scale components, also because it could allow the use of a cheaper and relatively more workable substrate (e.g. steel) and a more accurate optimization of the surface microstructure.

REFERENCES

[1]. P.D. Wood, H.E. Evans, C.B. Ponton, Investigation into the wear behaviour of Stellite6 during rotation as an unlubricated bearing at 600°C, Tribology International, article in press.

[2]. A. Gholipour, M. Shamanian, F. Ashrafizadeh, Microstructure and wear behaviour of Stellite 6 cladding on 17-4 PH stainless steel, Journal of Alloys and Compounds 509 (2011) 4905–4909.

[3]. W.S. da Silva, R.M. Souza, J.D.B. Mello, H. Goldenstein, Room temperature mechanical properties and tribology of NICRALC and Stellite casting alloys, Wear 271 (2011) 1819– 1827.

[4]. A. C. Kenneth, Wear resistance of cobalt base alloys, J. Metals 35 (1983) 52–60.

[5]. H. Berns: Microstructural properties of wear-resistant alloys, Wear 181-183 (1995) 271-279.

[6]. M.X. Yao, J.B.C.Wu, W. Xu, R. Liu, Metallographic study and wear resistance of a high-C wrought Co-based alloy Stellite 706K, Materials Science and Engineering: A 407 (2005) 291–298.

[7]. J.-N. Aoh,; C.J. Cheng, On the wear characteristics of cobalt-based hardfacing layer after thermal fatigue and oxidation, Wear 250 (2001) 611–620.

[8]. S. Hogmark, S. Jacobson, E. Coronel, On adhesion in tribological contacts – Causes and consequences. Tribologia, 26(1) (2007) 3–16.

[9]. S. Jacobson, S. Hogmark, Surface modifications in tribological contacts. Wear 266 (2009) 370-378.

[10]. M.W. Phaneuf: Applications of focused ion beam microscopy to materials science specimens. Micron 30 (1999) 277–288.

[11]. S.V. Prasad, J.R. Michael; T.R. Christenson, EBSD studies on wear-induced subsurface regions in LIGA nickel. Scripta Materialia 48 (2003) 255–260.

[12]. J. Li, M. Elmadagli, V.Y. Gertsman, J. Lo, A.T. Alpas, FIB and TEM characterization of subsurfaces of an Al–Si alloy (A390) subjected to sliding wear, Materials Science and Engineering A 421 (2006) 317–327.

[13]. J.J. Hu, R. Wheeler, J.S. Zabinski, P.A. Shade, A. Shiveley, A. A. Voevodin: Transmission Electron Microscopy Analysis of Mo–W–S–Se Film Sliding Contact Obtained by Using Focused Ion Beam Microscope and In Situ Microtribometer, Tribology Letters, Volume 32, Number 1 (2008) 49-57.

[14]. W. C. Oliver, G. M. Pharr, An improved technique for determining hardness and elastic modulus using load and displacement sensing indentation experiments, Journal of Materials Research 7 (1992) 1564-1583.

[15]. W. C. Oliver, G. M. Pharr, Measurement of hardness and elastic modulus by instrumented indentation: advances in understanding and refinements to methodology, Journal of Materials Research 19 (2004) 3-20.

[16]. F.J. Ulm, M. Vandamme, C. Bobko, J.A. Ortega, K. Tai, C. Ortiz, Statistical indentation techniques for hydrated nanocomposites: concrete, bone, and shale, J. Am. Ceram. Soc. 90 (9) (2007) 2677–2692.

[17]. G. Constantinides, F.J. Ulm, The nanogranular nature of C–S–H: J. Mech. Phys. Solids 55 (1), (2007) 64–90.

[18]. Y.Y. Santana, P.O. Renault, M. Sebastiani, J.G. La Barbera, J. Lesage, E. Bemporad, E. Le Bourhis, E.S. Puchi-Cabrera, M.H. Staia, Characterization and residual stresses of WC–Co thermally sprayed coatings, Surface & Coatings Technology 202 (2008) 4560–4565.

[19]. E. Bemporad, M. Sebastiani, M.H. Staia, E. Puchi Cabrera, Tribological studies on PVD/HVOF duplex coatings on Ti6Al4V substrate, Surface & Coatings Technology 203 (2008) 566–657.

[20]. M. Sebastiani, V. Mangione, D. De Felicis, E. Bemporad, F. Carassiti, Wear mechanisms and in-service surface modifications of a Stellite 6B Co-Cr alloy, Wear 290-291 (2012) 10-17